REACHABILITY ANALYSIS APPLIED TO SPACE SITUATIONAL AWARENESS

Marcus Holzinger
Graduate Research Assistant, Aerospace Engineering Sciences
University of Colorado at Boulder
Daniel Scheeres
Professor, Seebass Chair, Aerospace Engineering Sciences
University of Colorado at Boulder

Abstract

Several existing and emerging applications of Space Situational Awareness (SSA) relate directly to spacecraft Rendezvous, Proximity Operations, and Docking (RPOD) and Formation / Cluster Flight (FCF). Observation correlation of nearby objects, control authority estimation, sensor-track re-acquisition, formation re-configuration feasibility, 'stuck' thrusters, and worst-case passive safety analysis are some areas where analytical reachability methods have potential utility. Existing reachability theory is applied to RPOD and FCF regimes. Necessary conditions for maximum position reachability are developed, allowing for a reduction in reachable set computation dimensionality. The nonlinear relative equations of Keplerian motion are introduced and used for all reachable position set determinations. Examples for both circular and eccentric orbits are examined and compared. Weaknesses with the current implementation are discussed and future numerical improvements and analytical efforts are discussed.

1 Introduction

The concept of reachability is central to Space Situational Awareness (SSA), Rendezvous, Proximity Operations, and Docking (RPOD), and spacecraft Formation / Cluster Flight (FCF) applications. SSA can be broadly defined as knowing the location of objects in Earth orbit to specified accuracies as well as operational status, size, shape, and mission. With additional tracking capabilities coming online and improved sensor accuracy, the Space Object Catalog (SOC) is expected to grow by an order of magnitude [1]. With this marked increase in available data, analytical methods to evaluate Uncorrelated Tracks (UCTs) and maneuvering Resident Space Objects (RSOs) can significantly improve tractability of the SSA problem.

For RPOD and FCF applications, emerging mission concepts such as fractionation [2] drastically increase system complexity of on-board autonomous fault management systems. Reachability theory, as applied to SSA in RPOD and FCF applications, can involve correlation of nearby RSO observations, control authority estimation, and sensor track re-acquisition. Additional uses of reachability analysis are formation reconfiguration, worst-case passive safety, and propulsion failure modes such as a 'stuck' thruster.

When multiple spacecraft are in vicinity of one another with appreciable periods between observations, correlating new spacecraft tracks to previously known objects becomes a non-trivial problem. A particularly difficult sub-problem is seen when long breaks in observations are coupled with continuous, low-thrust maneuvers. Existing methods that are well suited to adaptation to this application involve applying generating functions to determine whether a new observation is reachable from a previous RSO track [3, 4, 5]. Reachability theory, related to generating functions, can compute contiguous reachability sets for known or estimated control authority to support such correlation efforts. Further, minimum required control authority may be estimated by determining optimal control trajectories between observations. In terms of reachability, this is equivalent to the new spacecraft observation lying on or near an outermost surface of a reachability set with an estimated minimum control authority. Lastly, in the event that spacecraft are

maneuvering within proximity of one another and sensor-track is lost, reachability analysis can predict the boundaries of the reachable space which must be searched for sensor re-acquisition.

With several spacecraft operating in a formation, a formation reconfiguration maneuver, particularly a fast and/or autonomous one, can be very complex. Reachability analysis can provide insight as to how a given formation geometry can reconfigure into any other geometry given time and thrust constraints. In the event of a spacecraft failure in a proximity operations scenario, it is desirable that spacecraft relative trajectories attenuate chance of a spacecraft collision. A maximal reachability set can be computed using worst-case unmodeled perturbations as an antagonistic control input to construct conservative passively safe relative trajectories or to make informed decisions regarding evasive maneuvers. One failure mode in RPOD scenarios that can prove particularly hazardous is that of a 'stuck' thruster. Such a thruster may have a solenoid valve 'stuck' in a permanent 'open' position, causing a continual thrust that may not be terminated. An applied reachability analysis of such a system can show the absolute maximum (or 'worst-case') state change that may result from such a failure over a fixed time. Such information can be applied to RPOD mission planning to minimize negative outcomes such as spacecraft collision.

Reachability theory has been extensively discussed in controls literature for both continuous and hybrid systems and is directly derived from optimal control theory [6, 7, 8, 9]. Polytopic reachability sets, which have straightforward parameterization and computation, have been shown to provide accurate conservative outer bounds for linear and norm-bounded nonlinear systems [10]. Through combining both ellipsoidal outter bounds as well as ellipsoidal inner bounds, exact reachability sets can be computed for convex reachability sets [11]. Reachability theory has also been successfully applied to differential games, specifically it has been applied to aircraft mid-air collision avoidance where one aircraft is avoiding another [12].

Applied specifically to RPOD, un-actuated reachability is relevant to the concept of Passive Safety (PS), defined as relative on-orbit trajectories that "guarantee collision avoidance with no thrusting required ... in the presence of a class of anomlous system behaviors" [13]. Currently, treatment of PS has been limited to ensuring that such drifting spacecraft do not deterministically [14, 15, 13] or statistically [16] collide with nearby spacecraft. These methods have similarities to existing reachability, where the spacecraft is essentially drifting and the possible states of the spacecraft are determined by the set of initial states and worst-case disturbances.

This paper reviews recent advances in reachability theory, applying them to the nonlinear relative orbit equations of motion, which are appropriate both for general SSA and spacecraft proximity operations applications. Lastly, reachability sets for several example scenarios are used to illustrate the behavior of systems with varying levels of control authority representative of existing operational spacecraft and propulsion technologies.

2 Applied Reachability Theory

Traditionaly, numerical solutions to Hamilton-Jacobi (HJ) PDE formulations are used to generate reachability sets for arbitrary nonlinear systems [17, 18]. Recent work suggests that significant computation reduction may be realized by individually solving for trajectories whose final states represent a sampling of the final reachability surface [19]. The results from this later work [19] are re-stated here, then used to generate some examples suitable for SSA applications. Given a nonlinear a differential system $\dot{\mathbf{x}} = f(\mathbf{x}, \mathbf{u}, t)$, with $\mathbf{x} \in \mathbb{R}^n$, $\mathbf{u} \in \mathbb{R}^m$, and $t \in [t_0, t_f]$, the state $\mathbf{x}$ and co-state $\mathbf{p}$ equations of motion are

$$\dot{\mathbf{x}} = f(\mathbf{x}, \mathbf{u}^*, t) \tag{1}$$

$$\dot{\mathbf{p}} = -\left(\frac{\partial \mathbf{f}}{\partial \mathbf{x}}^T\right)\mathbf{p} \tag{2}$$

where the optimal control policy $\mathbf{u}^*$ at any time $t > t_0$ is found to be

$$\mathbf{u}^* = u_m \frac{\frac{\partial \mathbf{f}}{\partial \mathbf{u}}^T \mathbf{p}}{\| \frac{\partial \mathbf{f}}{\partial \mathbf{u}}^T \mathbf{p} \|_2} \tag{3}$$

for any $\mathbf{u}$ in a norm-bounded set U (where u_m is the magnitude of the norm-bounding). The initial state $\mathbf{x}_0 = \mathbf{x}(t_0)$ is constrained to be within an ellopsoid, which is consistent with state knowledge obtained from probability distribution functions generated by operational orbit estimation algorithms [cite].

Definition 2.1 *Ellipsoidal Reachability Problem Statement (ERPS)*
A problem is an ERPS when there exists an initial reachability boundary condition ellipsoid $V(\boldsymbol{x}_0, t_0) = \boldsymbol{x}_0^T \boldsymbol{E} \boldsymbol{x}_0 - 1 \leq 0$, $\boldsymbol{E} \in \mathbb{S}_+^{n \times n}$, *dynamics* $\dot{\boldsymbol{x}} = \boldsymbol{f}(\boldsymbol{x}, \boldsymbol{u}, t)$, *and admissible control set* $\boldsymbol{u} \in U$, *where* U *is defined as*

$$U = \{\boldsymbol{u} \mid \boldsymbol{u}^T \boldsymbol{u} \leq u_m^2\} \tag{4}$$

where $u_m \in \mathbb{R}, u_m > 0$. *This definition of the admissible control set* U *is assumed for the remainder of this paper.*

Since this treatment considers ERPSs, the initial set of reachable states at time t_0 is defined as any $\mathbf{x}_0$ that satisfies

$$\mathbf{x}_0^T \mathbf{E} \mathbf{x}_0 - 1 \leq 0 \tag{5}$$

It is also assumed that the system in question satisfies the assumptions specified in definition 2.2.

Definition 2.2 *Class of Nonlinear Systems: Restricted Nonlinear Systems*
If a nonlinear systems under consideration has an optimal control $\boldsymbol{u}^*$ *that lies on the boundary of the feasible control set* U *and* $\boldsymbol{p}^T \left[\partial^2 \boldsymbol{f} / \partial \boldsymbol{u}^2\right] \geq 0$, *it is called a Restricted Nonlinear System (RNS).*

This assumption does not restrict the scope of these results in the context of SSA, as in orbital scenarios control and disturbances typically act on the objects as accelerations, producing a linear control (and hence, $\left[\partial^2 \mathbf{f} / \partial \mathbf{u}^2\right] = \mathbf{0}$ and $\mathbf{p}^T \left[\partial^2 \mathbf{f} / \partial \mathbf{u}^2\right] \geq 0$. To simplify notation and to emphasize the need to solve both $\mathbf{x}$ and $\mathbf{p}$ simultaneously, the state and adjoint dynamics are now concatenated into a larger state $\mathbf{z}$ such that

$$\mathbf{z} = \begin{bmatrix} \mathbf{x} \\ \mathbf{p} \end{bmatrix}$$

From which it follows that

$$\dot{\mathbf{z}} = \begin{bmatrix} \dot{\mathbf{x}} \\ \dot{\mathbf{p}} \end{bmatrix} = \mathbf{f}_z(\mathbf{x}, \mathbf{p}, t)$$

and

$$\mathbf{z}(t) = \phi_z(t; \mathbf{x}_0, \mathbf{p}_0, t_0) = \int_{t_0}^{t} \mathbf{f}_z(\mathbf{x}(\tau), \mathbf{p}(\tau), \tau) d\tau$$

with the initial conditions $\mathbf{x}(\tau = t_0) = \mathbf{x}_0$ and $\mathbf{p}(\tau = t_0) = \mathbf{p}_0$. It is also convenient to form the state and adjoint dynamic equations such that the velocity and position states can be written as:

$$\mathbf{x}^T = \begin{bmatrix} \mathbf{d}^T & \mathbf{v}^T \end{bmatrix}^T$$
$$\mathbf{p}^T = \begin{bmatrix} \mathbf{p}_d^T & \mathbf{p}_v^T \end{bmatrix}^T$$

With these definitions and assumptions complete, the maximum position reachability results are now introduced.

Given an ERPS with RNS dynamics, where $\mathbf{u}$ is in the norm-bounded set U, the absolute maximum position $\mathbf{d}_f$ at time t_f as well as the corresponding initial conditions $\mathbf{x}_0^T = [\mathbf{d}_0^T \ \mathbf{v}_0^T]$ satisfying (5) are found by solving the following system of equations [19]:

$$\begin{bmatrix} \mathbf{d}_f \\ \mathbf{d}_f \\ \mathbf{0} \end{bmatrix} = \mathbf{M} \phi_z(t_f; \mathbf{x}_0, -2\lambda \mathbf{E} \mathbf{x}_0, t_0) \tag{6}$$

$$\begin{bmatrix} \mathbf{d}_0 \\ \mathbf{v}_0 \end{bmatrix}^T \mathbf{E} \begin{bmatrix} \mathbf{d}_0 \\ \mathbf{v}_0 \end{bmatrix} - 1 = 0 \tag{7}$$

for $\mathbf{d}_0$, $\mathbf{v}_0$, $\mathbf{d}_f$, and λ, where

$$\mathbf{M} = \begin{bmatrix} \mathbb{I} & \mathbf{0} & \mathbf{0} & \mathbf{0} \\ \mathbf{0} & \mathbf{0} & \mathbb{I} & \mathbf{0} \\ \mathbf{0} & \mathbf{0} & \mathbf{0} & \mathbb{I} \end{bmatrix}_{\frac{3}{2}n \times 2n}$$

and λ is the Lagrange multiplier associated with the initial condition constraint (7). Similarly, if an a-priori direction is specified, then given an ERPS with RNS dynamics, where $\mathbf{u}$ is in the norm-bounded set U, and an initial position direction $\hat{\mathbf{d}}_0$ is specified, the absolute maximum reachable position $\mathbf{d}_f$ at time t_f as well as the corresponding initial direction magnitude d and velocity $\mathbf{v}_0$ satisfying (5) are found by solving the following equations:

$$\begin{bmatrix} \mathbf{d}_f \\ \mathbf{d}_f \\ \mathbf{0} \end{bmatrix} = \mathbf{M}\phi_z(t_f; \begin{bmatrix} d\hat{\mathbf{d}}_0 \\ \mathbf{v}_0 \end{bmatrix}, -2\lambda\mathbf{E}\begin{bmatrix} d\hat{\mathbf{d}}_0 \\ \mathbf{v}_0 \end{bmatrix}, t_0) \tag{8}$$

$$\begin{bmatrix} d\hat{\mathbf{d}}_0 \\ \mathbf{v}_0 \end{bmatrix}^T \mathbf{E} \begin{bmatrix} d\hat{\mathbf{d}}_0 \\ \mathbf{v}_0 \end{bmatrix} - 1 = 0 \tag{9}$$

for d, $\mathbf{v}_0$, $\mathbf{d}_f$, and λ.

Thus, solving equations (6) and (7) for $\zeta = [\mathbf{d}_0, \mathbf{v}_0, \mathbf{d}_f, \lambda]$ provides the maximum possible final position $\mathbf{d}_f$ starting from within the initial ellipsoid described by $\mathbf{x}_0^T\mathbf{E}\mathbf{x}_0 - 1 = 0$. This result can be used as a necessary condition for reachability - given some position observation $\tilde{\mathbf{d}}_f$ of an RSO at time t_f, if u_m is known then the observed position of the RSO must satisfy the following inequality:

$$\tilde{\mathbf{d}}_f^T\tilde{\mathbf{d}}_f \leq \mathbf{d}_f^T\mathbf{d}_f \tag{10}$$

This provides a straightforward, low-computation method of determining whether an observed RSO may possibly be a previously observed object. Similarly, if the new observation satisfies (10), then the exact reach set may be computed by discretizing the initial surface into $k^{n/2-1}$ initial directions $\hat{\mathbf{d}}_0$ and solving equations (8) and (9) for $\zeta_d = [d, \mathbf{v}_0, \mathbf{d}_f, \lambda]$.

2.1 Exact Nonlinear Relative Equations of Orbital Motion

Given an arbitrary reference orbit solution $\mathbf{x}_r(t)$, the reference radius (R_r), radius time derivative ($\dot{R}_r$), and true anomaly rate ($\dot{f}_r$) can be directly computed. In this case, the relative equations of motion can be written in the form $\dot{\mathbf{x}} = \mathbf{f}(\mathbf{x}, t) + \mathbf{B}\mathbf{u}$ [20]:

$$\dot{\mathbf{x}} = \begin{bmatrix} \dot{r} \\ \dot{s} \\ \dot{w} \\ \ddot{r} \\ \ddot{s} \\ \ddot{w} \end{bmatrix} = \begin{bmatrix} \dot{r} \\ \dot{s} \\ \dot{w} \\ 2\dot{f}_r\left(\dot{s} - s\frac{\dot{R}_r}{R_r}\right) + r\dot{f}_r^2 + \frac{\mu}{R_r^2} - \frac{\mu}{R^3}\left(R_r + r\right) \\ -2\dot{f}_r\left(\dot{r} - r\frac{\dot{R}_r}{R_r}\right) + s\dot{f}_r^2 - \frac{\mu}{R^3}s \\ -\frac{\mu}{R^3}w \end{bmatrix} + \begin{bmatrix} 0 & 0 & 0 \\ 0 & 0 & 0 \\ 0 & 0 & 0 \\ 1 & 0 & 0 \\ 0 & 1 & 0 \\ 0 & 0 & 1 \end{bmatrix} \begin{bmatrix} u_r \\ u_s \\ u_w \end{bmatrix} \tag{11}$$

and the inertial radius of the spacecraft is R, defined as

$$R = \sqrt{\left(R_r + r\right)^2 + s^2 + w^2}$$

$\partial\mathbf{f}/\partial\mathbf{x}$ can now be computed. The partial with respect to the control input, $\partial\mathbf{f}/\partial\mathbf{u}$, is simply

$$\frac{\partial\mathbf{f}}{\partial\mathbf{u}} = \mathbf{B} = \begin{bmatrix} \mathbf{0}_{3\times3} \\ \mathbb{I}_{3\times3} \end{bmatrix} \tag{12}$$

This provides the optimal control law $\mathbf{u}^*$ that is standard for systems with linear control:

$$\mathbf{u}^* = u_m \frac{\mathbf{B}^T \mathbf{p}}{\|\mathbf{B}^T \mathbf{p}\|} \tag{13}$$

The above results are now applied to specific examples.

3 Example Formulation

To illustrate the SSA applications of the results shown in this paper, 2-Degree-Of-Freedom (DOF) nonlinear relative motion dynamics (11) are formed into two examples. Because the cross-track (w) motion is only weakly coupled with the radial and along-track motion, the 2-DOF dynamics chosen for examination are those of radial (r) and along-track (s) motion.

3.1 Example 1: Spacecraft with Hall Thruster Propulsion System in LEO

This example illustrates the control authority of a LEO spacecraft equipped a Hall thruster propulsion system capable of providing 0.01N of thrust. Figs. 2(a) through 2(d) show the reachability surface at $t_f = P/4$, $P/2$, $3P/4$, and P (for example 1, $P = 5556s$).

Fig. 2(d) demonstrates the weakness of the control authority as well, as the final position reachability surface has already become significantly distorted by the dynamics at LEO. To provide a basis for comparison, Fig. 1 plots all four reachability surfaces with one another to provide additional perspective and insight into the growth of the reachability surface.

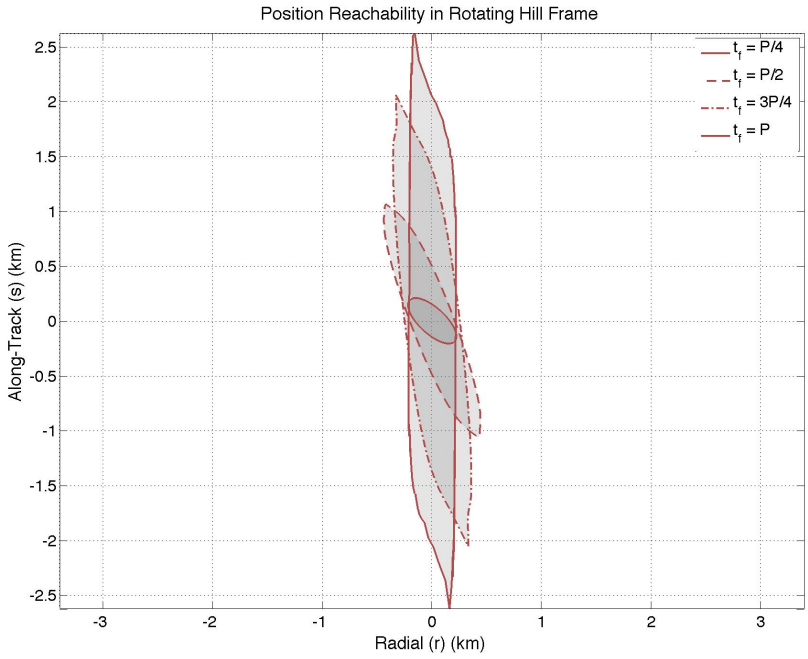

Figure 1: Example 1 Reachability for Select Time Intervals in a Rotating Hill Frame

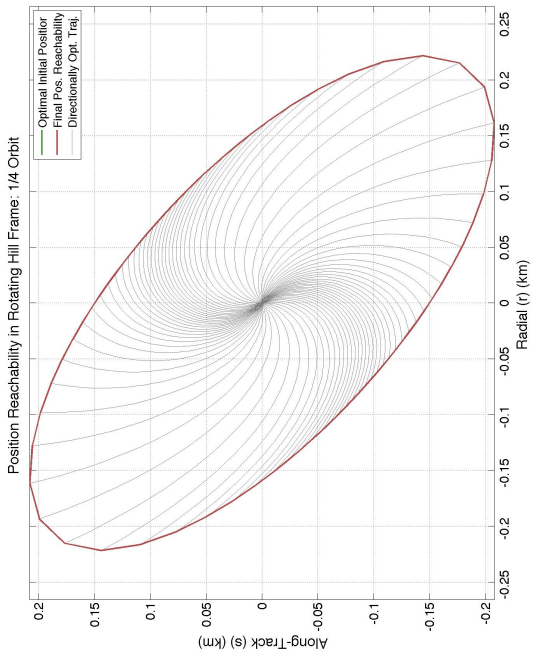

(a) $t_f = \frac{P}{4}$

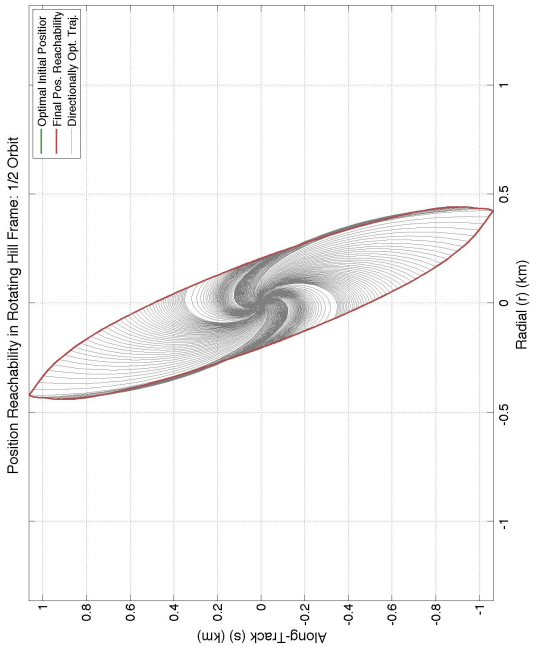

(b) $t_f = \frac{P}{2}$

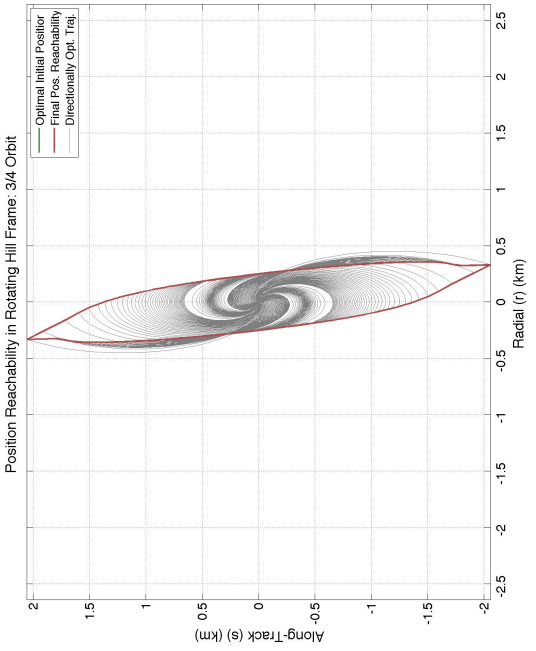

(c) $t_f = \frac{3P}{4}$

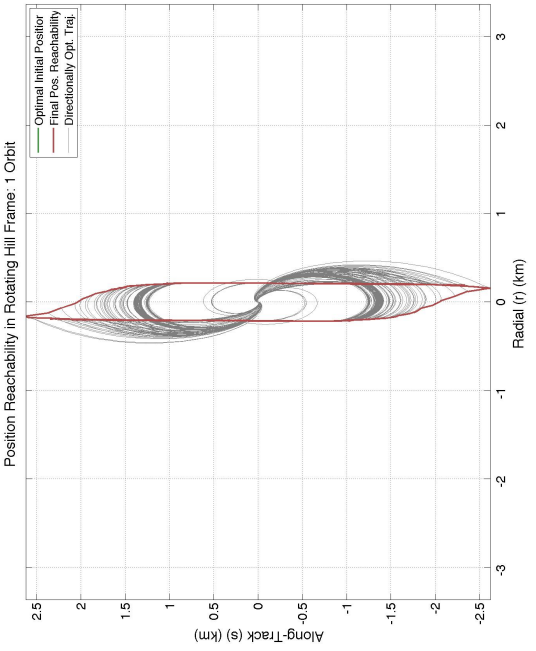

(d) $t_f = P$

Figure 2: Computed reachability sets for $t_f = P/4$, $P/2$, $3P/4$, and P. Note that later reachability sets (Fig. 2(c) and Fig. 2(d) are non-convex.

3.2 Example 2: Spacecraft with Hall Thruster Propulsion in LEO to GEO Transfer Orbit

This example illustrates the control authority of a spacecraft equipped with a Hall thruster propulsion system capable of providing 0.01N of thrust immediately after a burn injecting it into a LEO to GEO transfer orbit (400km altitude to 35,786km). Fig. 3 shows the reachability surface at $t_f = 1389s$ (equivalent to the half-orbit reachability plot from Example 1 shown in Fig. 2(b)).

Despite having the save level of control authority as Example 1, Example 2 resides in a transfer trajectory, and thus it's relative control authority increases as the orbit altitude increases. As a result, the position reachability surface at $t = 1389s$ in Fig. 3 is more 'spherical' than the reachability set for Example 1 shown in Fig. 2(b). For an easier comparison, the two are plotted together without individual trajectories in Fig. 4. For reference, Fig. 5 shows the reference orbit parameters, R

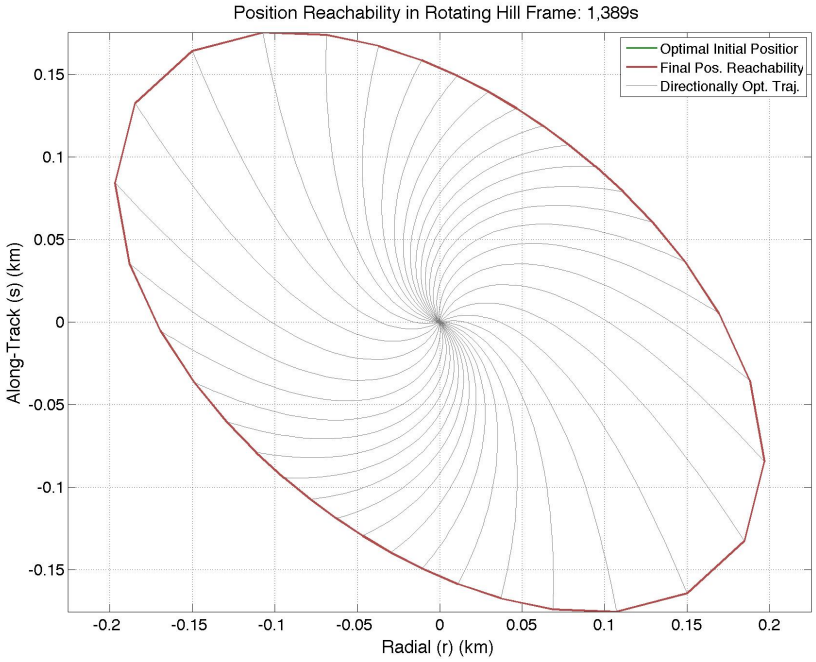

Figure 3: Example 2, $t_f = 1389s$

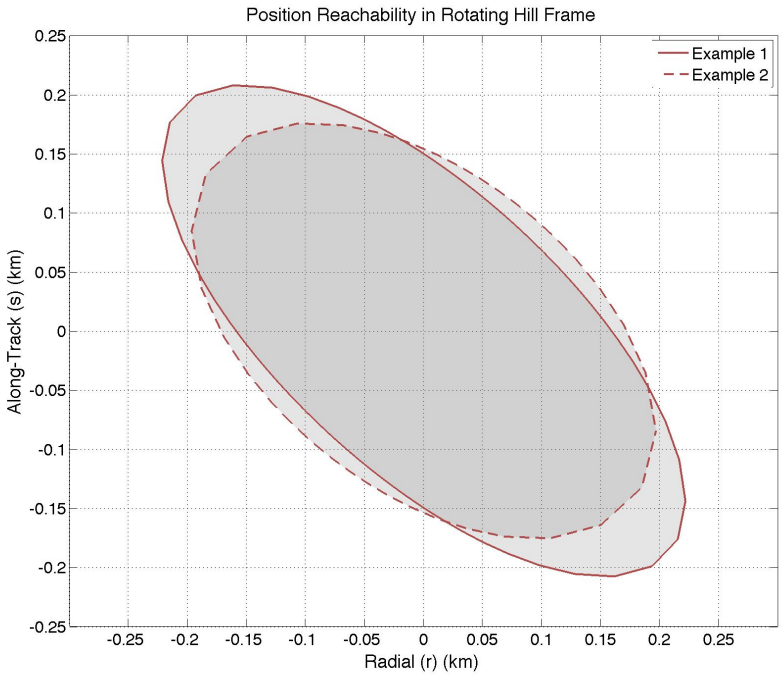

Figure 4: Comparison of reachability sets for Example 1 and Example 2 at $t_f = 1389s$.

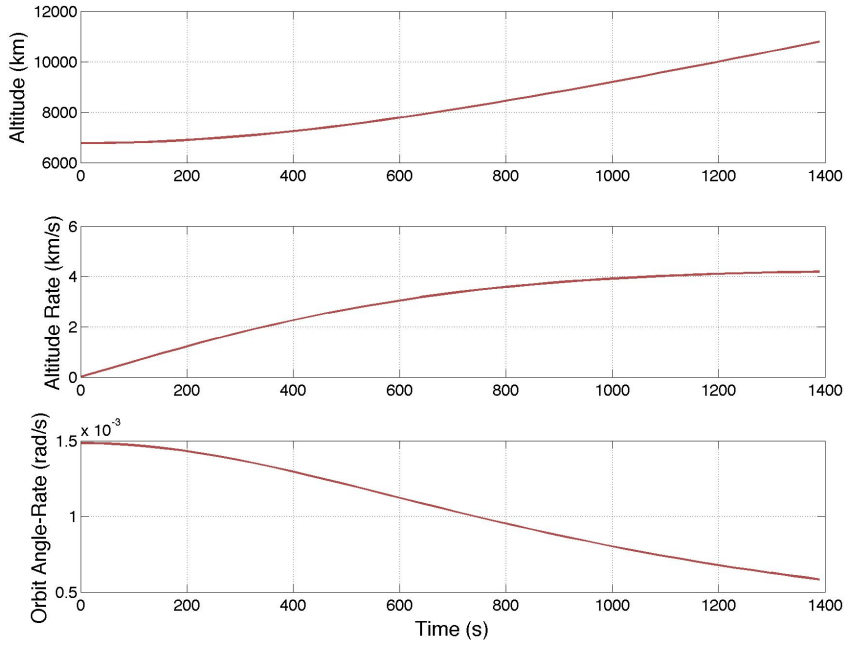

Figure 5: LEO to GEO reference orbit parameters R_r, $\dot{R}_r$, and $\dot{f}_r$

3.3 Summary of Results

Each example provides an illustration of what maximum position reachability surfaces look like at various time intervals. Unfortunately, because the integration method used requires the initial reachability set to be discretized, after a period of time the discretization resolution becomes insufficient, requiring certain initial directions to be discretized at different densities than other regions. Both significant compression and separation of the discretized trajectories occurs, causing the propagated surface to become coarse and angular in localized regions. This issue can be solved either by further increasing the discretization resolution or solving the original HJ PDE numerically [21].

Another problem encountered during the generation of the results was the appropriate selection of an initial guess for d, $\mathbf{v}_0$, $\mathbf{d}_f$, and λ. The current implementation uses the linear system to generate an initial guess, however this approach breaks down for larger time intervals and particularly eccentric orbits.

4 Conclusions

Existing reachability theory is particularly applicable to SSA and safety in both RPOD and FCF operations. Observation correlation, control authority characterization, target reacquisition, formation reconfiguration, 'stuck' thrusters, and worst-case passive safety may all be handled using analytical or numerical methods for reachability. Results from recent reachability advances were summarized and applied to a large class of nonlinear systems. The nonlinear equations of relative orbital motion are introduced in a rotating Hill frame for applications in proximity operations safety and SSA. For illustrative purposes, the Clohessy-Wiltshire (CW) equations are time- and distance-normalized to provide a basis for comparison of different scenarios at varying orbit altitudes, central bodies, and relative control authorities. The optimal control is examined in detail to provide insight into control direction 'switching.' Necessary and sufficient conditions for switching are developed and the implications of switching in various directions are examined. CW-coordinate normalization is leveraged to demonstrate control authority equivalence between example scenarios in both low Earth orbit and geostationary orbit. In each of the examples, the directional reachability equations are successfully solved for multiple initial directions and time intervals. Future work includes computing the reachability sets for a 3-DOF system, applying the theoretical results in this paper to a larger variety of SSA scenarios, exploring initial set discretization methods to more evenly populate points on the final reachability set, and identifying improved methods to generate initial guesses.

Acknowledgments

This work was supported by AFOSR Grant No. FA9550-08-1-0460.

References

[1] C. M. Cox, E. J. Degraaf, R. J. Wood, T. H. Crocker, "Intelligent Data Fusion for Improved Space Situational Awareness," AIAA Space 2005 Conference, Long Beach, 2005.

[2] O. Brown, P. Eremenko, "Fractionated Space Architectures: A Vision for Responsive Space," AIAA 4^{th} Responsive Space Conference, Los Angeles, 2006.

[3] V.M. Guibout and D.J.Scheeres, "Solving two-point boundary value problems using generating functions: Theory and Applications to optimal control and the study of Hamiltonian dynamical systems," University of Michigan, Ann Arbor, Michigan, Est. 2003.

[4] C. Park, V. Guibout, D. J. Scheeres, "Solving Optimal Continuous Thrust Rendezvous Problems with Generating Functions," Journal of Guidance, Control, and Dynamics, Vol. 29, No. 2, MarchApril 2006.

[5] C. Park, D. J. Scheeres, "Determination of optimal feedback terminal controllers for general boundary conditions using generating functions," Automatica 42 pp. 869 875. 2006.

[6] P. Varaiya, "Reach set computation using optimal control," Proceedings of the KIT Workshop on Verification of Hybrid Systems, pages 377-383, Grenoble, France, 1998.

[7] A. B. Kurzhanski, P. Varaiya, "Dynamic Optimization for Reachability Problems", Journal of Optimization Theory and Applications, Vol. 108, No. 2, pp 227-251, February 2001.

[8] J. Lygeros, "On the Relation of Reachability to Minimum Cost Optimal Control," IEEE Conference on Decision and Control, Las Vegas, December 2002.

[9] J. Lygeros, "On Reachability and Minimum Cost Optimal Control," Automatica 40, 2004.

[10] I. Hwang, D. M. Stipanovic, and C. J. Tomlin, "Applications of Polytopic Approximations of Reachable Sets to Linear Dynamic Games and a Class of Nonlinear Systems," Proceedings of the American Control Conference, Denver, Colorado, 2003.

[11] A. A. Kurzhanskiy, P. Varaiya, "Ellipsoidal Toolbox", Technical Report No. UCB/EECS-2006-46, Electrical Engineering and Computer Sciences, University of California at Berkeley, 2006.

[12] I. M. Mitchell, A. M. Bayen, and C. J. Tomlin, "A Time-Dependent Hamilton-Jacobi Formulation of Reachable Sets for Continuous Dynamic Games," IEEE Transactions on Automatic Control, Vol. 50, No. 7, July 2005

[13] L. S. Breger, J. P. How, "Safe Trajectories for Autonomous Rendezvous of Spacecraft," AIAA Guidance, Navigation, and Control Conference, August 2007, AIAA-2007-6860.

[14] M. Tillerson, G. Inalhan, J. P. How, "Co-ordination and Control of Distributed Spacecraft Systems using Convex Optimization Techniques," International Journal of Rubust and Nonlinear Control, 2002, 12:207-242.

[15] L. S. Breger, G. Inalhan, M. Tillerson, J. P. How, "Cooperative spacecraft Formation Flying: Model Predictive Control With Open And Closed-Loop Robustness," Modern Astrodynamics, Elsevier, Oxford, 2006.

[16] M. Holzinger, J. DiMatteo, J. Schwartz, M. Milam, "Passively Safe Receding Horizon Control for Satellite Proximity Operations," IEEE Conference on Decision and Control, Cancun, December 2008.

[17] W. H. Fleming, H. M. Soner, "Controlled Markov Processes and Viscosity Solutions, 2^{nd} Ed." New York, Springer, 2006

[18] D. F. Lawden, "Analytical Methods of Optimization," Mineola, NY, Dover Publications, 2003.

[19] M. Holzinger, D. Scheeres, "Applied Reachability for Space Situational Awareness and Safety in Spacecraft Proximity Operations," AIAA Guidance, Navigation, and Control Conference, August 2009, AIAA-2009-6096

[20] H. Schaub, J. L. Junkins, "Analytical Mechanics of Space Systems," Reston, VA, AIAA Educational Series, 2003.

[21] I. M. Mitchell, "A Toolbox of Level Set Methods," UBC Department of Computer Science Technical Report TR-2007-11, June 2007.